Mixing and chemical reaction at high Schmidt number near turbulent/nonturbulent interface in planar liquid jet

Cite as: Phys. Fluids **27**, 035114 (2015); https://doi.org/10.1063/1.4915510
Submitted: 24 July 2014 • Accepted: 06 March 2015 • Published Online: 26 March 2015

T. Watanabe, T. Naito, Y. Sakai, et al.

PHYSICS OF FLUIDS **27**, 035114 (2015)

Mixing and chemical reaction at high Schmidt number near turbulent/nonturbulent interface in planar liquid jet

T. Watanabe,[a] T. Naito, Y. Sakai, K. Nagata, and Y. Ito
Department of Mechanical Science and Engineering, Nagoya University, Nagoya, Japan

(Received 24 July 2014; accepted 6 March 2015; published online 26 March 2015)

This study investigates the mixing of reactive species at a high Schmidt number ($Sc \approx 600$) near the turbulent/nonturbulent (T/NT) interface in a planar liquid jet with a chemical reaction A + B → R. Reactants A and B are supplied from the jet and ambient flows, respectively. An I-type hot-film probe and optical fiber probe are used for the simultaneous measurements of the streamwise velocity, mixture fraction, and concentrations of all reactive species and for detecting the T/NT interface. Statistics conditioned on the time elapsed after interface detection are analyzed. The conditional mean mixture fraction and concentrations change sharply near the interface. The widths of these changes are independent of the chemical species. The conditional statistics reveal the dependence of the chemical reaction on the interface orientation. The segregation intensity near the interface shows that the mixing state of the two reactants also depends on the interface orientation. However, the large reaction rate near the interface is related to the large concentration of reactant A rather than the mixing state, because reactant A supplied from the jet tends to be deficient near the interface. Near the interface where the reaction rate is large, the concentration of the chemical product is also large. The difference in the product concentration between the different interface orientations is larger for the infinitely fast reaction (as investigated by using the equilibrium limit) than the finite Damköhler number case, and the dependence of the chemical reaction on the interface orientation is expected to be significant for a fast chemical reaction. © *2015 AIP Publishing LLC.* [http://dx.doi.org/10.1063/1.4915510]

I. INTRODUCTION

Recent studies have recognized the importance of the turbulent/nonturbulent (T/NT) interface,[1] which divides flow fields into turbulent and nonturbulent regions, in momentum and scalar transfers in free shear flows such as wakes, jets, and mixing layers. The turbulent and nonturbulent regions are distinguished by the existence of vorticity, and the vorticity magnitude changes sharply across the T/NT interface. The T/NT interface consists of two layers: turbulent sublayer[1] and viscous superlayer.[2] In the former, whose width is characterized by vortical structures near the interface, the vorticity magnitude changes sharply.[3] In the latter, whose thickness is of the order of the Kolmogorov scale η_K,[4] the vorticity is transferred from the turbulent region by viscous diffusion. Previous studies have investigated the entrainment process in free shear flows. Experiments on a T/NT interface in a round jet[5–7] showed that the entrainment process is dominated by small-scale eddies near the T/NT interface. Holzner *et al.* conducted experiments on oscillating-grid turbulence[8–10] and showed that the viscous process causes the local entrainment of nonturbulent fluids.[10] Recent increases in computational power have enabled researchers to elucidate the characteristics of the T/NT interface using direct numerical simulations (DNSs). For example, DNSs of a temporally

[a]Electronic mail: watanabe.tomoaki@c.nagoya-u.jp. Research Fellow of the Japan Society for the Promotion of Science.

developing jet[11] were used to investigate the thickness of the T/NT interface,[3] vortical structure,[12] kinetic energy budget near the T/NT interface,[13] and passive scalar mixing.[14] DNSs of a spatially developing jet[15] were also used to investigate the enstrophy and passive scalar transports,[16] enstrophy production mechanism,[17] and vortical structure[18] near the T/NT interface. These studies on the spatially developing jet revealed the importance of the interface orientation in the interface characteristics.

Turbulent mixing of chemical species can be seen in the environment and industrial equipment. It is important to control mixing and chemical reactions in engineering applications. The rate of fast chemical reactions is determined by the mixing process when the reaction timescale is small compared to the mixing timescale.[19] Thus, the relationship between mixing and reactions is important in modeling turbulent reactive flows. When two reactants are separately supplied by two flows, chemical reactions occur with their mixing in the interfacial region of the two flows.[20–22] The interfacial region of two reactants appears near the T/NT interface in free shear flows in which one reactant is contained in the turbulent fluid and the other, in the nonturbulent fluid. The reactant is entrained into the turbulent region with the local entrainment[10] of nonturbulent fluids near the T/NT interface.[16] The local entrainment also causes the spread of turbulent regions, which is responsible for the diffusion of chemical products. Thus, the characteristics of flow and scalar fields near the T/NT interface are important for chemical reactions in free shear flows. Because fast chemical reactions occur soon after reactants are mixed, the mixing process of chemical species near the interface is expected to be important for the modeling of turbulent reactive flows.[19]

One of the important parameters that characterize scalar mixing in turbulent flows is the Schmidt number $Sc \equiv \nu/D$, where ν and D are the kinematic viscosity and molecular diffusivity, respectively. The smallest scale of scalar fluctuations, called the Batchelor scale, is given by $\eta_B = \eta_K/Sc^{1/2}$. Thus, the Batchelor scale becomes small for scalar mixing at a high Schmidt number. In liquid flows, the Schmidt number is of the order of $10^2 - 10^3$ for the mixing of diffusive matter. Mixing in gaseous flows is characterized by a much smaller Schmidt number ($Sc \sim 1$). Thus, a wide range of Schmidt numbers can be observed in turbulent reactive flows, and therefore, turbulent reactive flows should be investigated for both large and small Schmidt numbers. Most previous studies on the T/NT interface focused on the characteristics of the flow and nonreactive scalar fields. On the other hand, reactive scalar fields near the T/NT interface have hardly been studied. The authors have investigated mixing and a chemical reaction near the T/NT interface at $Sc = 1$ using DNS of a planar jet with a second-order chemical reaction.[23] The Batchelor scale decreases in proportion to $Sc^{-1/2}$. Therefore, DNS of reactive flows at a high Schmidt number is almost infeasible because of the high computational cost. Turbulent reactive flows at a high Schmidt number have been investigated through experimental measurements of concentrations of chemical substances. Because most such flows contain multiple chemical substances, their concentrations must be measured simultaneously to investigate the chemical reactions in the flows. However, few measurement techniques can simultaneously measure concentrations of different substances in liquid flows. For a second-order chemical reaction $A + B \rightarrow P$, measurements of concentrations in reactive liquid flows have been conducted in a scalar mixing layer[24,25] and in a confined jet.[26–28] In these experiments, the laser-induced fluorescence technique is used for measuring concentrations in the fast acid-base neutralization reaction. Komori *et al.*[24] used the electrode conductivity technique for measuring concentrations for both moderately fast and fast reactions. We have also developed a concentration measurement system based on light absorption spectrometry[29,30] that can measure concentrations of multiple dyestuffs in liquid flows. This system was used for investigating a planar liquid jet with a reaction.[31–37] Although reactive liquid flows have been experimentally studied, mixing and chemical reactions near the T/NT interface have not been investigated.

This study aims to investigate the statistical properties of mixing and a chemical reaction at a high Schmidt number near the T/NT interface. Experiments are conducted for a planar liquid jet with a second-order chemical reaction $A + B \rightarrow R$. In this study, the streamwise velocity, mixture fraction, and concentrations of all reactive species are simultaneously measured by using an optical fiber probe based on light absorption spectrometry and an I-type hot-film probe. By detecting the T/NT interface using the time-series data of the instantaneous concentrations and velocity, the statistics of the concentrations and velocity are analyzed near the T/NT interface. Sec. II briefly

describes the concentration and velocity measurement in the reactive planar liquid jet. The T/NT interface is detected by using the detection method described in Sec. III. In Sec. IV, the statistics of the concentrations and velocity are analyzed. Finally, the conclusions are summarized in Sec. V.

II. SIMULTANEOUS MEASUREMENTS OF CONCENTRATION AND VELOCITY IN A PLANAR LIQUID JET WITH A SECOND-ORDER CHEMICAL REACTION

The planar liquid jet with a chemical reaction A + B → R investigated in this study is the same as in the previous study,[37] in which the details of the experiments, such as the experimental apparatus and parameters, were described. The aqueous solution for the jet contains the nonreactive species C and the reactant A, and the reactant B is contained in the ambient flow. The streamwise velocity U and concentrations of all species Γ_α (α = A, B, R, or C) are simultaneously measured by the I-type hot-film probe (TSI 1210-20W) and the optical fiber probe of the concentration measurement system,[32] whose detail is described in the previous papers.[36,37]

III. DETECTION OF THE T/NT INTERFACE

A. Detection of turbulent fluids

The T/NT interface is defined as the interface between the turbulent and the nonturbulent regions. The intermittency function[38,39] $I(t)$ is defined by

$$I(t) \equiv \begin{cases} 1 & \text{for a turbulent fluid} \\ 0 & \text{for a nonturbulent fluid} \end{cases}, \tag{1}$$

which is determined by thresholding a criterion function.[40] The vorticity magnitude is often used as a criterion function for $I(t)$ in DNSs.[3,4,12,13,16–18,41–44] Because the measurement of the vorticity vector is not easy, a passive scalar, such as temperature[38] and concentration,[5–7,45,46] is often used as a marker of turbulent fluids in experimental studies. The velocity data obtained by particle image velocimetry (PIV)[47,48] and hot-wire anemometry[40,49] were also used to detect turbulent fluids.

In the present experiment, the time-series data of concentrations $\Gamma_\alpha(t)$ and streamwise velocity $U(t)$ are obtained at measurement locations, and $I(t)$ is calculated from a criterion function defined using $\Gamma_\alpha(t)$ and $U(t)$. Two different intermittency functions are calculated for the time-series data obtained by the optical fiber probe and hot-film probe. As in the previous studies,[5–7,45,46] $\Gamma_\mathrm{C}(t)$ is used as a marker of turbulent fluids. Then, the intermittency function $I_\mathrm{C}(t)$ is given by

$$I_\mathrm{C}(t) = \begin{cases} 1 & (\Gamma_\mathrm{C}(t) \geq \Gamma_\mathrm{th}(\boldsymbol{x})) \\ 0 & (\Gamma_\mathrm{C}(t) < \Gamma_\mathrm{th}(\boldsymbol{x})) \end{cases}. \tag{2}$$

Here, $\Gamma_\mathrm{th}(\boldsymbol{x})$ is the interface detection threshold and is a function of the location $\boldsymbol{x} = (x, y, z)$, where x, y, and z are the streamwise, cross-streamwise, and spanwise coordinates, respectively. In this study, $\Gamma_\mathrm{th}(\boldsymbol{x}) = 0.05\langle\Gamma_\mathrm{C}\rangle_\mathrm{C}$ is used as the threshold, where $\langle\ \rangle_\mathrm{C}$ is the mean (time-averaged) value on the jet centerline. Thus, $\Gamma_\mathrm{th}(\boldsymbol{x})$ changes in the streamwise direction but is independent of the cross-streamwise and spanwise locations. According to Hedley and Keffer[40] and Terashima *et al.*,[49] $U(t)$ is also used to detect turbulent fluids, and the following function calculated from the time derivative of $U(t)$ is used as the criterion function $C_U(t)$ for detecting turbulent fluids:

$$C_U(t) = \frac{1}{2}\left(|\dot{U}(t)| + \frac{\sqrt{\langle\dot{U}^2\rangle}}{\sqrt{\langle\ddot{U}^2\rangle}}|\ddot{U}(t)|\right). \tag{3}$$

Here, $\dot{U}$ and $\ddot{U}$ are the first and second derivatives of $U(t)$ with time t, respectively. In the previous experiments,[40,49] $C_U(t)$ smoothed by a low-pass filter is used for calculating the intermittency function $I_U(t)$,

$$I_U(t) = \begin{cases} 1 & (C_U(t) \geq C_{U\mathrm{th}}(\boldsymbol{x})) \\ 0 & (C_U(t) < C_{U\mathrm{th}}(\boldsymbol{x})) \end{cases}. \tag{4}$$

Here, $C_{U\mathrm{th}}(\boldsymbol{x})$ is the interface detection threshold. After $C_U(t)$ for frequencies higher than 100 Hz is filtered out in the Fourier space, $I_U(t)$ is calculated from Eq. (4). In this study, $C_{U\mathrm{th}}(\boldsymbol{x}) = 0.096\langle U\rangle_{\mathrm{C}}^2/b_U$ is used as the threshold, where b_U is the jet half-width based on the mean streamwise velocity. Similar to $\Gamma_{\mathrm{th}}(\boldsymbol{x})$, $C_{U\mathrm{th}}(\boldsymbol{x})$ depends solely on the streamwise location.

The choice of the thresholds is important for detecting the T/NT interface. When the thresholds are too small, nonturbulent fluids are incorrectly detected as turbulent ones because of nonzero values of $\Gamma_{\mathrm{C}}(t)$ and $C_U(t)$ arising from experimental noise. Therefore, the thresholds should be larger than the values arising from experimental noise. Fortunately, $\Gamma_{\mathrm{C}}(t)$ shows a large discrepancy between turbulent and nonturbulent fluids, as can be seen in Westerweel *et al.*[7] Similarly, it was also confirmed that the threshold level has small influence on the turbulent zone detected by the criterion functions defined by the time derivative of velocity when the threshold is not too small.[40] Therefore, values of $\Gamma_{\mathrm{C}}(t)$ and $C_U(t)$ that are slightly larger than the nonturbulent values are reasonable choices for the thresholds. We set the thresholds so that nonzero values of $\Gamma_{\mathrm{C}}(t)$ and $C_U(t)$ arising from experimental noise are not incorrectly detected as turbulent fluids. We confirmed that the thresholds have small influence on the results (Appendix).

B. Detection of the T/NT interface

The intermittency function changes from 0 to 1 or 1 to 0 when the T/NT interface passes through the measurement location. Therefore, $I_{\mathrm{C}}(t)$ and $I_U(t)$ are used for detecting the T/NT interface. Because the T/NT interface is strongly convoluted, the interface faces various directions. The characteristics of the T/NT interface depend on the interface orientation.[16–18] In this study, the concentrations and streamwise velocity near the T/NT interface are investigated separately for different interface orientations.

Figure 1 shows the schematic of the T/NT interface in a planar jet. The sampling volumes of the optical fiber probe and the hot-film probe are separated from each other in the cross-streamwise direction with a distance of $\delta = 0.65$ mm. We investigate the leading edge, which faces the streamwise (x) direction, and the trailing edge, which faces the direction opposite to the x direction. The turbulent fluids are located upstream (downstream) of the leading (trailing) edge. Therefore, the intermittency function changes from 0 to 1 (from 1 to 0) when the leading (trailing) edge passes

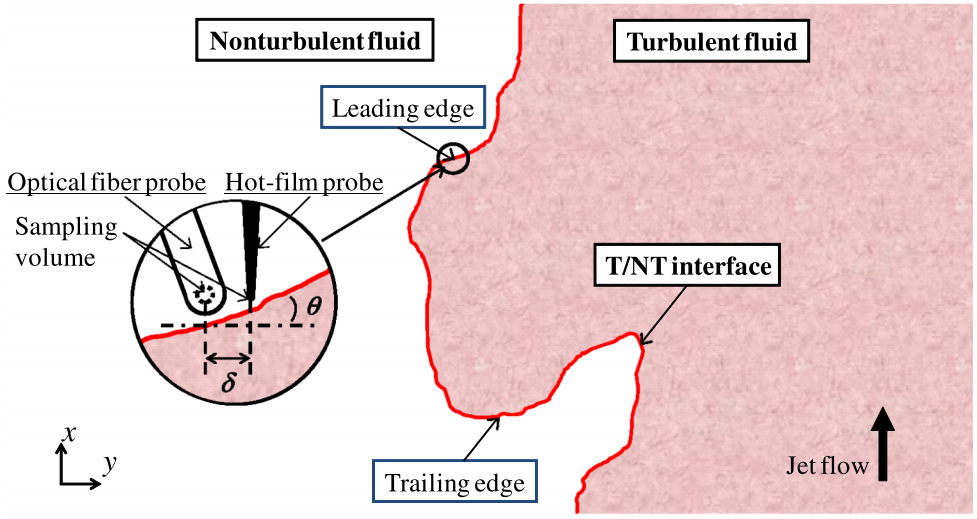

FIG. 1. Schematic of the T/NT interface in a planar jet. The leading and trailing edges are detected by using the time-series data of concentrations and streamwise velocity measured by the optical fiber probe and hot-film probe. The relationship between the positions of the two probes and the interface is also shown.

through the probe location. When the T/NT interface passing through the probe locations is parallel to the cross-streamwise direction, the changes in $I_C(t)$ and $I_U(t)$ are simultaneously detected by the optical fiber probe and hot-film probe. However, because most interfaces are inclined, there is a time lag in the interface detection time between the two probes. The angle of the interface inclination (θ) is defined in Fig. 1. We use the detected interface for investigating the leading and trailing edges when the angle $|\theta|$ is smaller than 15°, where $|\theta|$ is estimated from

$$|\theta| = \tan^{-1}\left(\frac{U(t_{U0})|t_{C0} - t_{U0}|}{\delta}\right). \tag{5}$$

Here, $I_C(t)$ and $I_U(t)$ change at $t = t_{C0}$ and t_{U0}, respectively. $U(t_{U0})$ is the streamwise velocity at the interface detection time t_{U0}. The criterion for defining the leading and trailing edges is 25° in the previous DNS,[16–18,44] and the criterion of 15° used in this study is relatively more rigorous. We compared the conditional statistics, which are defined in Subsection III C, calculated using two different criteria: 15° and 25°. It was confirmed that the difference between the two criteria has small influence on the conditional statistics.

Because the convolutions of the T/NT interface can be related to the large vorticity structures,[3] the distance between the two probes should be smaller than the length scale associated with these structures for discriminating the interface orientations. The radius of the large vorticity structures near the T/NT interface in a jet is almost equal to the Taylor microscale.[3] The distance between the two probes is smaller than the Taylor microscale,[37] and is sufficiently small for discriminating the interface orientations. When the T/NT interface is detected by one probe, but not by another probe, the detected T/NT interface is discarded from the analysis. Thus, the velocity criteria by Eq. (4) prevent concentration fluctuations far from the actual T/NT interface defined by vorticity from being misdetected as the T/NT interface.

C. Definitions of averages

The statistics are calculated by taking three types of averages: "mean," "turbulent mean," and "conditional mean." The "mean" value of the measured time-series signal $f(t)$, denoted by $\langle f \rangle$, is calculated by taking the conventional time-average of $f(t)$. The "turbulent mean" value of $f(t)$, denoted by $\langle f \rangle_T$, is the average of f in the turbulent region,[39] and is calculated by $\langle f \rangle_T = \langle I_C(t) f(t) \rangle / \gamma_C$, where the intermittency factor $\gamma_C = \langle I_C \rangle$ is the probability that fluids are turbulent.

Because the single-point measurements are conducted in this study, the statistics conditioned on the distance from the T/NT interface are not available unlike in the experiments using PIV[48] or planar laser-induced fluorescence.[5–7,45,46] Therefore, the time elapsed from the interface detection time is used for defining the conditional statistics. Hereafter, the time elapsed from t_{C0} is denoted by Δt. The "conditional mean" value of $f(t)$, denoted by $\langle f \rangle_I$, is the mean value of f conditioned on Δt for the detected interface. We also use the conditional probability density function (pdf) $p_f(f; \Delta t)$, which is the pdf of f calculated from the data that are sampled after Δt from t_{C0}. These conditional statistics are calculated for the leading and trailing edges.

The measurements for the statistics based on the mean and turbulent mean values are conducted over 21 s, which is sufficiently long for obtaining the converged statistics.[35] The cross-streamwise profiles of statistics are investigated at three streamwise locations: $x/d = 10$, 20, and 40, where d is the width of the jet inlet and the origin of the coordinate system is located at the center of the jet nozzle. For investigating the T/NT interface, the measurements are conducted at the same three streamwise locations at a fixed cross-streamwise location where the interface can be frequently detected. The cross-streamwise location of the measurement is determined from γ, as shown in Sec. IV. For investigating the interface, the simultaneous measurements of concentrations and velocity are conducted over 84 s. These measurements are repeated four times. The conditional statistics are obtained from these four measurements.

IV. RESULTS AND DISCUSSIONS

A. Statistical properties of concentrations of reactive species in turbulent region

The statistics based on time-averaged values were investigated in the previous studies.[32,34,35,37] The measurement results of the velocity and concentration of C were compared with the DNS of a planar jet,[16–18] and it was confirmed that the self-similar profiles of the velocity and concentration statistics show good agreement between the experiment and DNS. Here, we investigate the concentration statistics in the turbulent region by using statistics based on turbulent mean values. Figure 2 shows the cross-streamwise profiles of the intermittency factors $\gamma_C = \langle I_C \rangle$ and $\gamma_U = \langle I_U \rangle$. For reference, Fig. 2 also shows the intermittency factor obtained by the DNS of a planar jet,[16] in which the turbulent fluids are detected by using the vorticity magnitude. The cross-streamwise profiles of γ_C and γ_U are similar to the DNS results. We investigate the statistics based on turbulent mean values in the region where γ_C exceeds 0.05. In Fig. 2, the vertical broken line shows the cross-streamwise location of $y/b_U = 1.7$ ($y/b_\xi \approx 1.2$), at which the measurements for investigating the T/NT interface are conducted.

For the second-order reaction A + B → R, the chemical reaction rate is given by

$$S_R = -S_A = -S_B = k\Gamma_A\Gamma_B. \tag{6}$$

Here, S_α (α = A, B, or R) is the chemical source term for reactive species α, which appears in the transport equation of Γ_α, and k is the reaction rate constant. The reaction rate cannot be defined for the equilibrium limit because this limit represents the state in which one of the two reactants is completely consumed by the reaction.[37] The reaction rate normalized by d, the velocity difference at $x = 0$ ($U_J - U_A$), and the maximum product concentration under the stoichiometric condition (Γ_{R0}) is $\hat{S}_R = Da\hat{\Gamma}_A\hat{\Gamma}_B$, where U_J is the mean bulk velocity at the jet nozzle, U_A is the mean bulk velocity of the ambient flow, $\hat{\Gamma}_\alpha$ is the concentration normalized by $\Gamma_{\alpha 0}$ ($\Gamma_{\alpha 0}$: initial concentration for α = A, B, or C), and $Da = k(\Gamma_{A0} + \Gamma_{B0})d/(U_J - U_A)$ is the Damköhler number. In the present experiment, $Da = 11.7$.[37]

Figure 3 shows the turbulent mean concentration of product R, $\langle \Gamma_R \rangle_T$, and the turbulent mean reaction rate, $\langle \hat{S}_R \rangle_T$. The concentrations in the frozen (nonreactive case) and equilibrium limits (infinitely fast reaction)[37,50] are compared with the finite Damköhler number case. The profiles show that product R is distributed and the chemical reaction occurs in the entire turbulent region. The reaction proceeds rapidly at $x/d = 10$ near the jet centerline, which is far from the T/NT interface. Therefore, in the downstream (x) direction, $\langle \Gamma_R \rangle_T$ near the jet centerline rapidly increases. Thus, in the downstream region, a large concentration of the chemical product can be observed near the jet centerline rather than the edge.

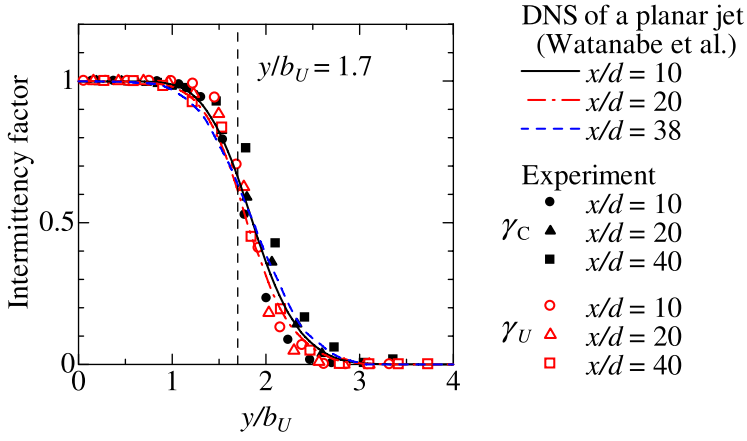

FIG. 2. Intermittency factors obtained from the concentrations and streamwise velocity measurements. The intermittency factors are compared with the DNS results by Watanabe *et al.*[16]

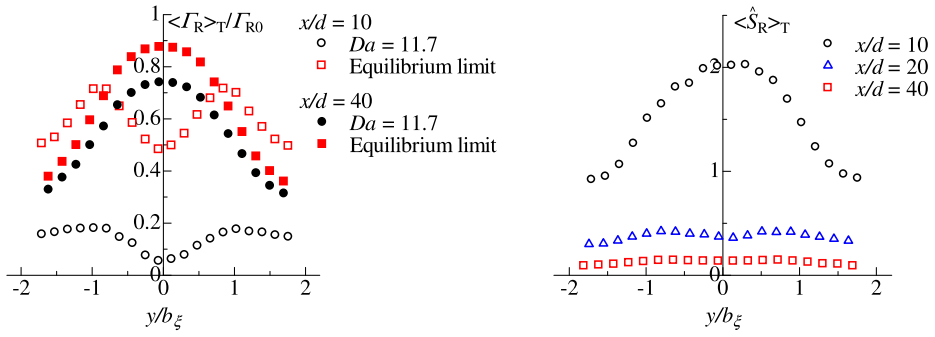

(a) Turbulent mean concentration of product R (b) Turbulent mean reaction rate

FIG. 3. Cross-streamwise profiles of (a) turbulent mean concentration of product R and (b) turbulent mean reaction rate.

B. Conditional mean mixture fraction and velocity near the T/NT interface

Figures 4(a) and 4(b) show the conditional mean mixture fraction $\langle\xi\rangle_I$ for the leading and trailing edges, respectively, where the mixture fraction ξ is calculated by $\xi = \Gamma_C/\Gamma_{C0}$. The interface detection time by the concentration signal is represented by $\Delta t = 0$. Near the leading (trailing) edge, the turbulent fluids are located upstream (downstream) of the interface, as shown in Fig. 1. Therefore, positive (negative) Δt corresponds to the turbulent region near the leading (trailing) edge. The mean streamwise velocity $\langle U\rangle$ and Taylor microscale based on the turbulent mean values, $\lambda_T = \sqrt{\langle u''^2\rangle_T/\langle(\partial u''/\partial x)^2\rangle_T}$, are used to normalize Δt. Here, $u'' = U - \langle U\rangle_T$ is the fluctuating component of the streamwise velocity from the turbulent mean value and the spatial derivative is calculated by using the Taylor hypothesis of a frozen turbulence. Figure 4 shows that the nonturbulent region consists of ambient fluids, for which the mixture fraction is defined as 0. Near the trailing edge, $\langle\xi\rangle_I$ gradually increases toward the deep inside of the turbulent region while it sharply increases near the leading edge. A similar difference between the two interfaces can be seen in the DNS of a planar jet.[16] A sharp jump in $\langle\xi\rangle_I$ can be observed from $|\Delta t|\langle U\rangle/\lambda_T = 0$ to $|\Delta t|\langle U\rangle/\lambda_T \approx 1$, whose width is considered to be close to the Taylor microscale. The DNSs of planar jets also show that the conditional mean scalar changes sharply near the T/NT interface, and the width of the change is nearly equal to the Taylor microscale.[14,16] $\langle\xi\rangle_I$ in the turbulent region is different between the leading and the trailing edges, and $\langle\xi\rangle_I$ near the trailing edge is smaller than that near the leading edge. The difference in ξ between these two interfaces can be important in the chemical reaction because Γ_A and Γ_B strongly depend on ξ. A mixture fraction smaller than its stoichiometric value $\xi_S = 0.333$[37] means that reactant A supplied from the jet is deficient. Figure 4 shows that reactant

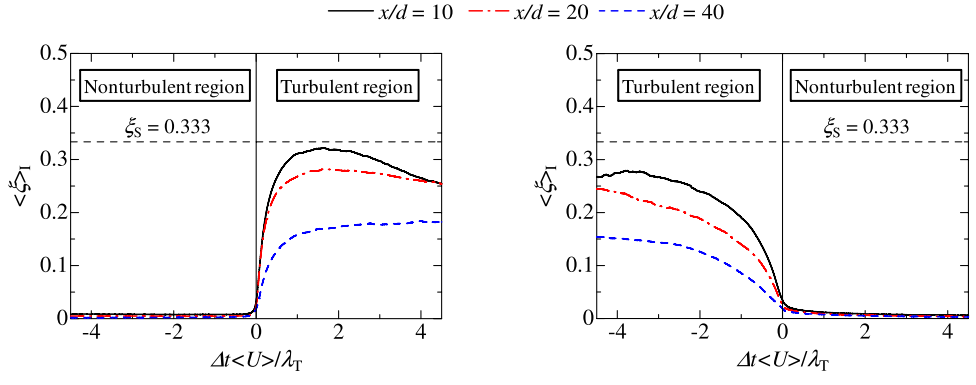

(a) Leading edge (b) Trailing edge

FIG. 4. Conditional mean mixture fraction: (a) leading edge and (b) trailing edge. The stoichiometric value of the mixture fraction[37] $\xi_S = 0.333$ is shown by a lateral broken line.

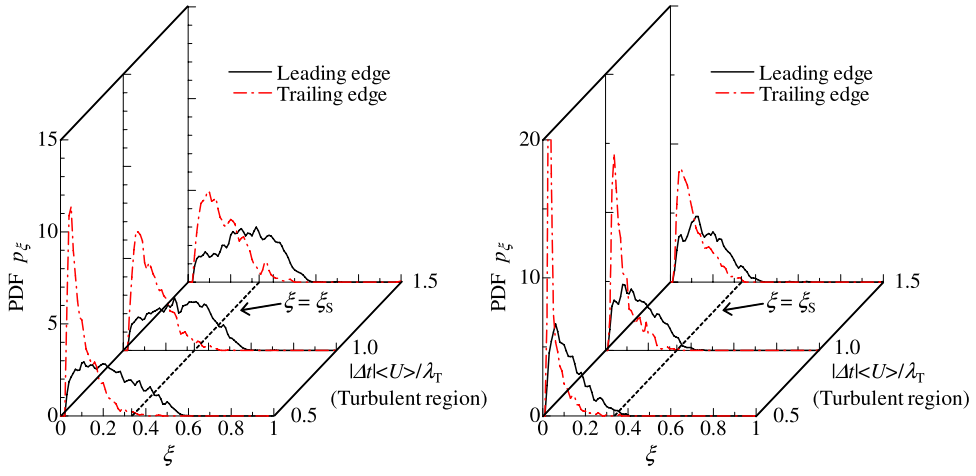

(a) $x/d = 20$ (b) $x/d = 40$

FIG. 5. Conditional probability density function of the mixture fraction in the turbulent region ($|\Delta t|\langle U\rangle/\lambda_T = 0.5$, 1.0, and 1.5) near the leading ($\Delta t > 0$) and trailing ($\Delta t < 0$) edges: (a) $x/d = 20$; (b) $x/d = 40$. The broken line indicates the stoichiometric value of the mixture fraction[37] ($\xi_S = 0.333$).

A is deficient near the interfaces on average ($\langle\xi\rangle_I < \xi_S$). The mixture fraction near the interfaces decreases as x increases. This is because the ambient (nonturbulent) fluids with $\xi = 0$ are entrained into the turbulent region across the interfaces with jet development.

Figure 5 shows the conditional pdf of ξ, $p_\xi(\xi; \Delta t)$, in the turbulent region. As $|\Delta t|$ increases, p_ξ has a large value for a larger mixture fraction. Near the trailing edge, a large peak of p_ξ can be observed for small ξ, and a large probability of p_ξ appears for a mixture fraction smaller than ξ_S. However, both larger and smaller ξ than ξ_S can be observed near the leading edge at $x/d = 20$. Thus, except for the turbulent region near the leading edge in the upstream region, reactant A is deficient in the turbulent region near the T/NT interface.

Figure 6(a) shows the conditional mean streamwise velocity $\langle U\rangle_I$. For comparing the two interfaces, $\langle U\rangle_I$ obtained for the leading edge is shown with $-\Delta t$ instead of Δt. Therefore, the left side in this figure corresponds to the turbulent region. The change in $\langle U\rangle_I$ is not as steep as that in $\langle\xi\rangle_I$ in Fig. 4. In a jet flow, the turbulent fluid is characterized by a faster streamwise velocity than the nonturbulent fluid.[7,18] One can observe this tendency of the streamwise velocity in Fig. 6(a), and

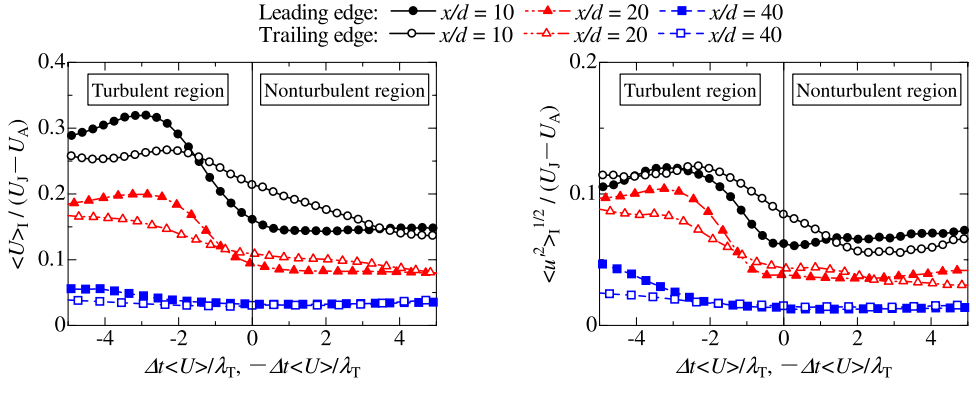

(a) Conditional mean velocity (b) Conditional rms velocity

FIG. 6. (a) Conditional mean streamwise velocity and (b) conditional rms velocity near the leading and trailing edges detected at $x/d = 10$, 20, and 40. Conditional statistics obtained for the leading edge are shown with $-\Delta t$. Lines with closed symbols: leading edge. Lines with open symbols: trailing edge.

$\langle U\rangle_{\mathrm{I}}$ in the turbulent region is faster than that in the nonturbulent region. The difference in $\langle U\rangle_{\mathrm{I}}$ between the turbulent and the nonturbulent regions is significant near the leading edge in the upstream region (x/d = 10 and 20), in agreement with the DNS of a spatially developing planar jet.[18] This difference becomes small at x/d = 40 because the streamwise velocity in the turbulent core region decays in the downstream direction. In the DNS of a planar jet,[18] the leading and trailing edges were distinguished by considering the three-dimensional geometry of the interface. In contrast, in the present experiment, the interface orientation is examined only on the x-y plane. Although there are differences in the method to calculate the conditional statistics between the experiment and the DNS, the conditional mean velocity in the experiment shows a similar trend to the DNS results.[18]

Figure 6(b) shows the conditional rms streamwise velocity $\langle u'^2\rangle_{\mathrm{I}}^{1/2}$, where $u' = U - \langle U\rangle_{\mathrm{I}}$ is the fluctuating component of U from $\langle U\rangle_{\mathrm{I}}$. In the present conditional analysis, the interface is assumed to pass the probe location in the streamwise direction, as shown in Fig. 1, although there are three-dimensional movements of the interface. The velocity of the interface movement can be represented by the sum of the fluid velocity and interface propagation velocity (local entrainment velocity).[10,16] Because the interface propagation velocity is of the order of the Kolmogorov velocity,[51] the fluid velocity has a larger contribution to the interface movement. From Fig. 6, it is found that $\langle u'^2\rangle_{\mathrm{I}}^{1/2}$ is smaller than $\langle U\rangle_{\mathrm{I}}$, and the mean velocity has a larger contribution to the interface movement in the streamwise direction than the fluctuating component. Taveira *et al.* showed that the conditional rms spanwise velocity is small compared with the streamwise and cross-streamwise components in a temporally developing planar jet.[13] Therefore, because of the absence of the mean spanwise velocity, it can be considered that the spanwise velocity of the interface movement is smaller than the streamwise velocity. Thus, as considered in Fig. 1, the interface tends to move in the streamwise direction rather than the spanwise direction.

C. Conditional mean concentrations near the T/NT interface

Figures 7–9 show the conditional mean concentrations $\langle \Gamma_\alpha\rangle_{\mathrm{I}}$ of A, B, and R near the leading and trailing edges, respectively. The conditional mean concentrations satisfy the following:[37]

$$\frac{\langle \Gamma_{\mathrm{A}}\rangle_{\mathrm{I}}}{\Gamma_{\mathrm{A0}}} + \frac{\langle \Gamma_{\mathrm{B}}\rangle_{\mathrm{I}}}{\Gamma_{\mathrm{B0}}} + \frac{\langle \Gamma_{\mathrm{R}}\rangle_{\mathrm{I}}}{\Gamma_{\mathrm{R0}}} = 1. \tag{7}$$

The conditional profiles show that the nonturbulent fluid solely consists of unreacted reactant B, and reactant A and product R are contained in the turbulent region. This means that the spread of the chemical product arises from the development of turbulent regions, which is caused by the diffusion of vorticity near the interface. The conditional mean concentrations sharply change from

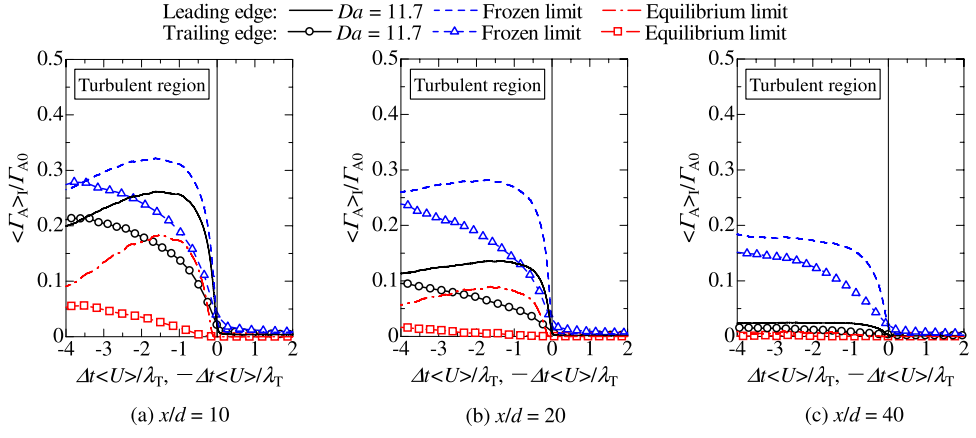

FIG. 7. Conditional mean concentrations of reactant A for $Da = 11.7$, the frozen limit, and the equilibrium limit near the leading and trailing edges. Conditional statistics obtained for the leading edge are shown with $-\Delta t$: (a) $x/d = 10$, (b) $x/d = 20$, and (c) $x/d = 40$.

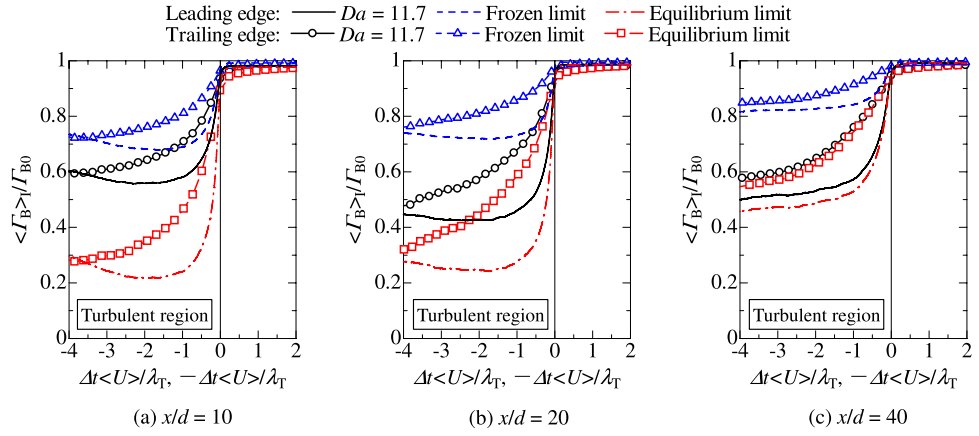

FIG. 8. Same as Fig. 7, but for reactant B.

the interface ($\Delta t = 0$) toward the turbulent region. Similar to $\langle\xi\rangle_\mathrm{I}$ in Fig. 4, the change in $\langle\Gamma_\alpha\rangle_\mathrm{I}$ near the leading edge is steeper than that near the trailing edge. Note that the width of the large change in $\langle\Gamma_\alpha\rangle_\mathrm{I}$ near the interface is almost independent of the reactive species and whether the reaction occurs. In the turbulent region near the interface, reactive species A, B, and R coexist; however, the concentrations of reactant A and product R in the turbulent region decrease toward the T/NT interface.

The dependence of the reaction near the interface on the Damköhler number is investigated by comparing $\langle\Gamma_\alpha\rangle_\mathrm{I}$ among the finite Damköhler number $Da = 11.7$, frozen limit, and equilibrium limit. In Figs. 7 and 8, the difference between the reactive and the nonreactive cases increases as x increases, and the chemical reaction proceeds in the streamwise direction. Near the leading edge at $x/d = 40$ and near the trailing edge, $\langle\Gamma_\mathrm{A}\rangle_\mathrm{I}$ in the equilibrium limit is very small even in the turbulent region. In the equilibrium limit,[37] concentration of A is equal to 0 when ξ is smaller than ξ_S. As shown in the pdf of ξ (Fig. 5), ξ is frequently smaller than ξ_S near the leading edge in the downstream region and near the trailing edge. Therefore, in these regions, reactant A hardly exists when the infinitely fast reaction occurs. For reactant B, $\langle\Gamma_\mathrm{B}\rangle_\mathrm{I}$ in the turbulent region is larger near the trailing edge than the leading edge. In the turbulent region near the interface, $\langle\Gamma_\mathrm{B}\rangle_\mathrm{I}$ in the frozen limit increases with x because the ambient fluid, which contains reactant B, is entrained into the turbulent region. However, $\langle\Gamma_\mathrm{B}\rangle_\mathrm{I}$ for $Da = 11.7$ decreases in the turbulent region from $x/d = 10$ to 20 because there the reactant B reacts with reactant A [Figs. 8(a) and 8(b)]. In the further downstream region [Figs. 8(b) and 8(c)], $\langle\Gamma_\mathrm{B}\rangle_\mathrm{I}$ for the reactive case increases in the downstream direction.

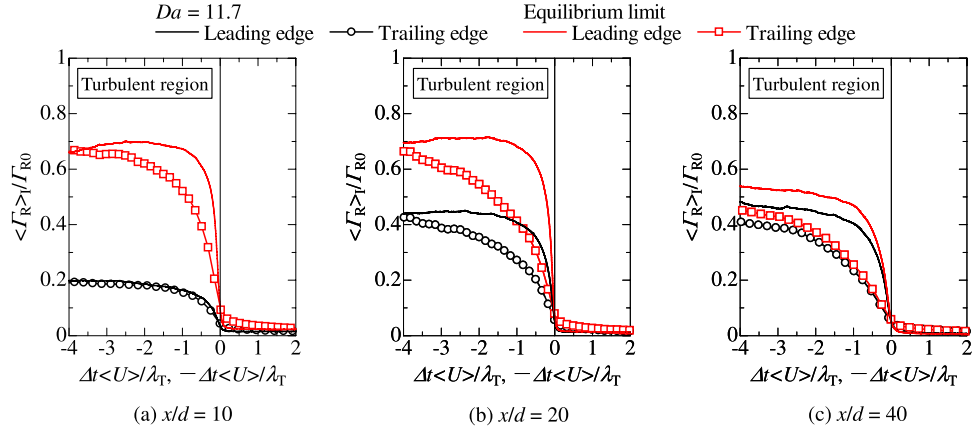

FIG. 9. Same as Fig. 7, but for product R.

In the downstream region, Γ_A for the reactive case is small because of the chemical consumption of A. Therefore, reactant B is entrained from the nonturbulent region without reacting with reactant A.

From Fig. 9, it is found that $\langle \Gamma_R \rangle_I$ near the leading edge is larger than that near the trailing edge. The turbulent fluids near the trailing edge contain only a small amount of A. Because the concentration of A is large near the leading edge, much more product R is produced near the leading edge than the trailing edge. Note that this difference is larger in the equilibrium limit than the finite Damköhler number case ($Da = 11.7$). Therefore, the dependence of the chemical reaction on the interface orientation is expected to be significant for a fast chemical reaction.

D. Conditional mean reaction rate near the T/NT interface

The conditional mean reaction rate $\langle \hat{S}_R \rangle_I = Da \langle \hat{\Gamma}_A \hat{\Gamma}_B \rangle_I$ is shown in Fig. 10 for the leading and trailing edges. It is found that the chemical reaction occurs mainly in the turbulent region. From the interface ($\Delta t = 0$), the conditional mean reaction rate sharply increases toward the turbulent region. Upon comparing $\langle \hat{S}_R \rangle_I$ between the leading and the trailing edges, one can see that the reaction rate is large near the leading edge. It is also found that as with the conditional mean concentrations, the jump in $\langle \hat{S}_R \rangle_I$ is steeper near the leading edge. Thus, the large reaction rate near the leading edge is expected to result in a large concentration of product R in the turbulent region near the leading edge in Fig. 9. Because of the chemical consumption of the reactants, a large reaction rate near the interface is observed in the upstream region.

The reactive planar jet at $Sc = 1$ investigated in the DNS[15,23] is very similar to the planar liquid jet in the present experiment except for the Schmidt number. It was shown that the product concentration and reaction rate near the trailing edge tend to be smaller than those near other interfaces.[23] A similar tendency is observed in the conditional statistics in the present experiment ($Sc \approx 600$). Thus, the dependence of the concentrations and reaction rate on the interface orientation is similar for high and low Schmidt numbers of the reactive species.

The conditional mean reaction rate $\langle S_R \rangle_I$ is represented by

$$\langle S_R \rangle_I = k \langle \Gamma_A \rangle_I \langle \Gamma_B \rangle_I + k \langle \gamma'_A \gamma'_B \rangle_I \tag{8}$$

$$= k \langle \Gamma_A \rangle_I \langle \Gamma_B \rangle_I (1 + I_{SI}). \tag{9}$$

Here, $\gamma'_\alpha = \Gamma_\alpha - \langle \Gamma_\alpha \rangle_I$ is the fluctuating component of Γ_α from the conditional mean value. The conditional segregation intensity I_{SI} is defined by

$$I_{SI} \equiv \frac{\langle \gamma'_A \gamma'_B \rangle_I}{\langle \Gamma_A \rangle_I \langle \Gamma_B \rangle_I}. \tag{10}$$

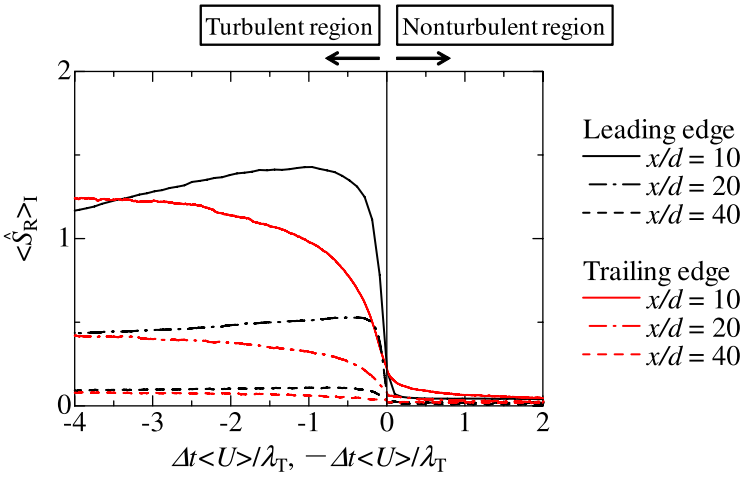

FIG. 10. Conditional mean reaction rate near the leading and trailing edges at $x/d = 10$, 20, and 40. Conditional statistics obtained for the leading edge are shown with $-\Delta t$.

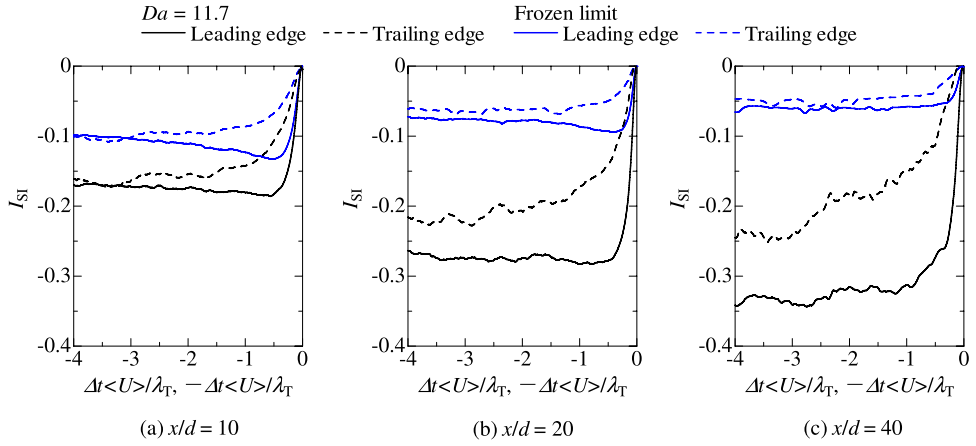

FIG. 11. Conditional segregation intensity in the turbulent region near the leading and trailing edges. Conditional statistics obtained for the leading edge are shown with $-\Delta t$: (a) $x/d = 10$, (b) $x/d = 20$, and (c) $x/d = 40$.

Similar to the conventional segregation intensity,[19,25] I_{SI} has a negative value between -1 and 0: when the two reactants do not coexist, they are fully segregated ($I_{SI} = -1$) while $I_S = 0$ when they are completely and ideally mixed. Thus, I_{SI} can be considered a measure of the unmixedness of the two reactants near the T/NT interface, and suppresses $\langle S_R \rangle_I$. Figure 11 shows I_{SI} in the turbulent region. Because $\langle \Gamma_A \rangle_I$ is close to 0 in the nonturbulent region, the turbulent region, where both reactants are contained, is shown in Fig. 11. In the equilibrium limit, the concentration of one of the two reactants is 0, and therefore, $I_{SI} = -1$. Thus, I_{SI} is compared between $Da = 11.7$ and the frozen limit. In the frozen limit, I_{SI} near the interface increases in the x direction, indicating that the mixing of A and B proceeds. From I_{SI} for $Da = 11.7$ and the frozen limit, it is clear that the chemical reaction reduces I_{SI} because the presence of the chemical product causes the two reactants to be segregated.[25] I_{SI} is different between the leading and the trailing edges. I_{SI} near the leading edge is small, and the difference between the reactive and the nonreactive cases is large near the leading edge. Therefore, for $Da = 11.7$, I_{SI} near the leading edge is much smaller than its value near the trailing edge. The segregation intensity decreases owing to the chemical reaction because of the chemical product. Therefore, the large difference in I_{SI} between the reactive and the nonreactive cases near the leading edge is related to the large concentration of product R.

The conditional segregation intensity I_{SI} shows that the mixing of the two reactants is close to the ideal mixing state ($I_{SI} = 0$) near the trailing edge compared with the leading edge. Therefore, the unmixedness of the two reactants significantly suppresses the conditional mean reaction rate near the leading edge. However, $\langle \hat{S}_R \rangle_I$ is larger near the leading edge. $\langle \hat{S}_R \rangle_I$ can be represented by

$$\langle \hat{S}_R \rangle_I = Da \langle \hat{\Gamma}_A \rangle_I \langle \hat{\Gamma}_B \rangle_I (1 + I_{SI}). \tag{11}$$

Therefore, the large reaction rate near the leading edge is related to a large value of the product of conditional mean concentrations $\langle \hat{\Gamma}_A \rangle_I \langle \hat{\Gamma}_B \rangle_I$. From the relationship among Γ_A, Γ_B, and Γ_R,[37] $\langle \hat{\Gamma}_A \rangle_I \langle \hat{\Gamma}_B \rangle_I$ can be written by

$$\langle \hat{\Gamma}_A \rangle_I \langle \hat{\Gamma}_B \rangle_I = \langle \hat{\Gamma}_A \rangle_I (1 - \langle \hat{\Gamma}_R \rangle_I - \langle \hat{\Gamma}_A \rangle_I) = -\left(\langle \hat{\Gamma}_A \rangle_I - \frac{1 - \langle \hat{\Gamma}_R \rangle_I}{2} \right)^2 + \frac{(1 - \langle \hat{\Gamma}_R \rangle_I)^2}{4} \tag{12}$$

$$= \langle \hat{\Gamma}_B \rangle_I (1 - \langle \hat{\Gamma}_R \rangle_I - \langle \hat{\Gamma}_B \rangle_I) = -\left(\langle \hat{\Gamma}_B \rangle_I - \frac{1 - \langle \hat{\Gamma}_R \rangle_I}{2} \right)^2 + \frac{(1 - \langle \hat{\Gamma}_R \rangle_I)^2}{4}. \tag{13}$$

Thus, $\langle \hat{\Gamma}_A \rangle_I \langle \hat{\Gamma}_B \rangle_I$ is a quadratic function of $\langle \hat{\Gamma}_A \rangle_I$ and $\langle \hat{\Gamma}_B \rangle_I$. Equations (12) and (13) imply that for a fixed value of $\langle \hat{\Gamma}_R \rangle_I$, $\langle \hat{\Gamma}_A \rangle_I \langle \hat{\Gamma}_B \rangle_I$ becomes maximum on the condition $\langle \hat{\Gamma}_A \rangle_I = \langle \hat{\Gamma}_B \rangle_I = (1 - \langle \hat{\Gamma}_R \rangle_I)/2$. It is also found that as $\langle \hat{\Gamma}_R \rangle_I$ increases, $\langle \hat{\Gamma}_A \rangle_I \langle \hat{\Gamma}_B \rangle_I$ decreases because the increase in $\langle \hat{\Gamma}_R \rangle_I$ is caused by the chemical reaction, which reduces the concentrations of the reactants.

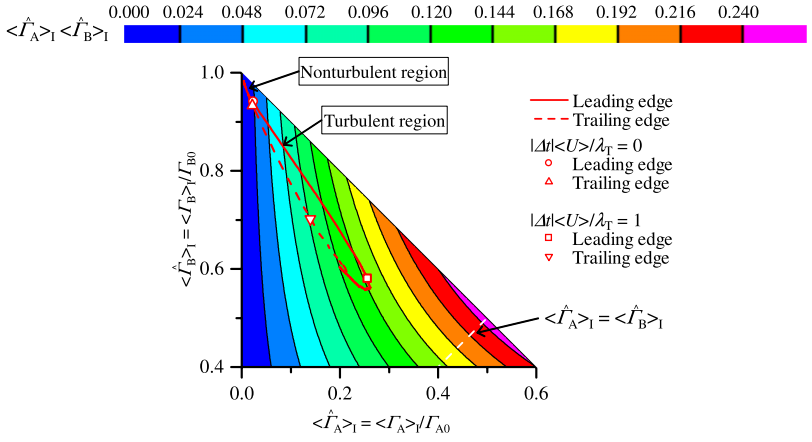

FIG. 12. Trajectory of $\langle \hat{\Gamma}_A \rangle_I$ and $\langle \hat{\Gamma}_B \rangle_I$ in their associated phase map obtained for the interface at $x/d = 10$. The trajectory from the nonturbulent region where $|\Delta t|\langle U \rangle/\lambda_T = 2$ toward the turbulent region where $|\Delta t|\langle U \rangle/\lambda_T = 4$ is shown for the leading and trailing edges. The region where $\langle \hat{\Gamma}_A \rangle_I + \langle \hat{\Gamma}_B \rangle_I > 1$ is not shown because $(\langle \hat{\Gamma}_A \rangle_I, \langle \hat{\Gamma}_B \rangle_I)$ in this region does not satisfy Eq. (7). In the phase map, a value of $\langle \hat{\Gamma}_A \rangle_I \langle \hat{\Gamma}_B \rangle_I$ corresponding to a given $(\langle \hat{\Gamma}_A \rangle_I, \langle \hat{\Gamma}_B \rangle_I)$ is visualized by the color map. The interface detection time $|\Delta t|\langle U \rangle/\lambda_T = 0$ and the turbulent region corresponding to $|\Delta t|\langle U \rangle/\lambda_T = 1$ are shown by red open symbols. The white broken line shows $\langle \hat{\Gamma}_A \rangle_I = \langle \hat{\Gamma}_B \rangle_I$.

Figure 12 shows the trajectory of $\langle \hat{\Gamma}_A \rangle_I$ and $\langle \hat{\Gamma}_B \rangle_I$ in their associated phase map near the leading and trailing edges at $x/d = 10$. $\langle \hat{\Gamma}_A \rangle_I$ and $\langle \hat{\Gamma}_B \rangle_I$ shown in Figs. 7(a) and 8(a) are replotted in this figure. In the nonturbulent region, the conditional mean concentrations are in the region close to $(\langle \hat{\Gamma}_A \rangle_I, \langle \hat{\Gamma}_B \rangle_I) \approx (0, 1)$, where $\langle \hat{\Gamma}_A \rangle_I \langle \hat{\Gamma}_B \rangle_I$ is small. Toward the turbulent region across the interface, $(\langle \hat{\Gamma}_A \rangle_I, \langle \hat{\Gamma}_B \rangle_I)$ in the phase map moves to the region where $\langle \hat{\Gamma}_A \rangle_I \langle \hat{\Gamma}_B \rangle_I$ is large. In the turbulent region where $|\Delta t|\langle U \rangle/\lambda_T = 1$, $(\langle \hat{\Gamma}_A \rangle_I, \langle \hat{\Gamma}_B \rangle_I)$ near the leading edge is located in the region with larger $\langle \hat{\Gamma}_A \rangle_I \langle \hat{\Gamma}_B \rangle_I$ than that near the trailing edge. In Fig. 12, $\langle \hat{\Gamma}_A \rangle_I$ is smaller than $\langle \hat{\Gamma}_B \rangle_I$ near the interface, and this tendency is clearly observed near the trailing edge. Because of the large $\langle \hat{\Gamma}_A \rangle_I$, the trajectory of $(\langle \hat{\Gamma}_A \rangle_I, \langle \hat{\Gamma}_B \rangle_I)$ near the leading edge appears close to the line of $\langle \hat{\Gamma}_A \rangle_I = \langle \hat{\Gamma}_B \rangle_I$. Thus, the large concentration of reactant A near the leading edge causes the large $\langle \hat{\Gamma}_A \rangle_I \langle \hat{\Gamma}_B \rangle_I$, which makes the conditional mean reaction rate large.

A larger amount of reactant A is contained near the leading edge than the trailing edge. This difference in Γ_A might be explained by considering the velocity field near the interface. Reactant A is supplied from the jet, and its concentration is large in the turbulent region away from the interface. The streamwise velocity is the velocity component normal to the leading and trailing edges. The turbulent region is characterized by the faster streamwise velocity than the location of the interface (Fig. 6). The geometry of the interfaces (see Fig. 1) shows that the turbulent fluid is located in the upstream and downstream of the leading and trailing edges, respectively. Therefore, the turbulent fluid near the interface is transferred toward the leading edge, but it relatively moves away from the trailing edge. The turbulent fluid, which contains a large amount of A, is transferred toward the leading edge, resulting in the large $\langle \hat{\Gamma}_A \rangle_I$ near the leading edge. The concentration of product P is also large in the turbulent core region. Similar to reactant A, the streamwise velocity can transfer product P toward the leading edge, and $\langle \hat{\Gamma}_P \rangle_I$ becomes larger near the leading edge. Because only the streamwise velocity is available in the present measurement, the transport in the direction parallel to the interface is unknown. However, the difference in the transport by the streamwise velocity between the leading and the trailing edges can be one of the factors that cause the concentration statistics, such as the mean concentration, mean mixture fraction, and mean reaction rate, to differ between the two interfaces.

The present experiment is conducted for a slow chemical reaction. Therefore, although the results in Fig. 10 show that the chemical reaction proceeds more rapidly near the leading edge, it cannot be concluded whether a fast reaction depends on the interface orientation in mixing in the jet at high Schmidt number. However, we can presume the dependence of fast reactions on the interface orientation from the characteristics of the scalar dissipation rate of the mixture

fraction $N = D(\nabla\xi \cdot \nabla\xi)$ in turbulent flows. Previous studies have shown that sheet-like structures are formed in regions with large scalar dissipation rate.[52–56] Because there is a large scalar gradient in the interface normal direction near the interface, as in Fig. 4, a sheet-like structure appears in the turbulent region near the interface.[57] This structure is well modeled by a simple one-dimensional unsteady strained laminar diffusion-layer model.[58] The scalar dissipation rate is affected by turbulent fields, especially via a strain field.[52,53] The diffusion-layer model shows that the compressive and extensive strains in the scalar gradient direction make the layer thin and thick, respectively. In turbulent flows, the diffusion layer tends to align orthogonally to the compressive strain. Note that the scalar dissipation rate increases as the diffusion layer becomes thinner. The strain field near the T/NT interface strongly depends on the interface orientation in the planar jet, and the compressive strain near the leading edge acts in the interface normal direction more frequently than near the trailing edge.[17] Therefore, the diffusion-layer model indicates that a thinner diffusion layer with larger scalar dissipation rate appears near the leading edge. Indeed, this tendency was observed in the conditional mean scalar dissipation profile in the DNS of a planar jet.[23] It is well known that the large reaction rate of fast chemical reactions is linked to the region with large scalar dissipation rate.[59] Therefore, similar to the slow reaction, fast reactions proceeds more rapidly near the leading edge than the trailing edge. This dependence of a fast chemical reaction on the interface orientation was observed in the DNS results of a reactive jet for the low Schmidt number case ($Sc = 1$).[23] The interface orientation dependence of the strain field is related to the motion of the turbulent fluid relative to the interface movement.[17] When the turbulent fluid approaches the interface, the compressive strain acts in the interface normal direction. This is frequently observed near the leading edge because the turbulent fluid with fast streamwise velocity is located in the upstream of the interface. In contrast, for the opposite motion of the turbulent fluid, which can be often seen near the trailing edge, the compressive strain does not act in the interface normal direction.

It should be noted that the difference in the streamwise velocity between the turbulent and the nonturbulent regions is caused by the mean flow in the jet. The mean flow in the jet makes the relative motion of the turbulent fluid different between the leading and the trailing edges and causes the interface orientation dependence of the scalar transport and dissipation characteristics, which are important in mixing and chemical reactions in turbulent flows. Therefore, the interface orientation effect on the reaction rate is expected to be significant in the upstream region because the streamwise velocity in the turbulent region decays in the streamwise direction.

V. CONCLUDING REMARKS

The mixing of reactive species at a high Schmidt number ($Sc \approx 600$) near the T/NT interface is investigated in a planar liquid jet with a chemical reaction A + B → R. Reactants A and B are supplied from the jet and ambient flows, respectively. The statistics in the turbulent region show that the chemical reaction occurs and the chemical product is distributed in the entire turbulent region, and the reaction rate is large near the jet centerline away from the T/NT interface.

The T/NT interface is detected by using the intermittency functions obtained from the time-series data of the concentrations and velocity. The statistics conditioned on the time elapsed from the interface detection time are analyzed for the leading and trailing edges. The conditional mean mixture fraction and concentrations sharply change near the interface. The width of these changes is independent of the chemical species. The mixture fraction in the turbulent region near the interface is significantly different between the leading and the trailing edges, and the mixture fraction is much smaller near the trailing edge. The difference in the mixture fraction between the two interfaces causes the dependence of the chemical reaction on the interface orientation. In the present experiment, a mixture fraction smaller than its stoichiometric value is frequently observed near the trailing edge. Therefore, the concentration of reactant A is close to 0 near the trailing edge when the infinitely fast reaction occurs. The concentration of reactant B near the interface can increase by the entrainment of the ambient fluid when reactant B is entrained without reacting with A after most of A near the interface has reacted.

The mixing of the two reactants is close to ideal near the trailing edge compared with the leading edge. However, the conditional mean reaction rate is larger near the leading edge than the trailing edge. It is found that the large reaction rate near the leading edge can be related to the large concentration of the deficient reactant A rather than the mixing state. Because of the large reaction rate near the leading edge, the conditional mean concentration of the chemical product is also large near the leading edge. The difference in the conditional mean product concentration between the leading and the trailing edges is larger in the equilibrium limit than in the finite Damköhler number case. This result indicates that the dependence of the chemical reaction on the interface orientation is expected to be significant for a fast chemical reaction.

The turbulent fluid is characterized by faster streamwise velocity than the nonturbulent fluid. Because the leading and trailing edges face opposite directions, the fast streamwise velocity in the turbulent region makes the scalar transport different between these two interfaces. Near the leading edge, the turbulent fluid with large concentrations of A and P is transferred toward the leading edge. This transfer of the turbulent fluid can be related to the large concentrations of A and P near the leading edge, and the large concentration of A causes a large reaction rate. Thus, the scalar transfer by the velocity field near the T/NT interface can be important in the chemical reaction near the interface.

ACKNOWLEDGMENTS

The authors would like to thank Dr. O. Terashima for his help in this study. This work was supported by JSPS KAKENHI Grant No. 25002531 and MEXT KAKENHI Grant Nos. 25289030, 25289031, and 25630052.

APPENDIX: INFLUENCE OF THE CHOICE OF INTERFACE DETECTION THRESHOLDS

Here, we examine the influence of the choice of interface detection thresholds on the conditional statistics. The thresholds $\Gamma_{\rm th}$ and $C_{U\rm th}$ are used for the intermittency functions defined in

TABLE I. Thresholds used in the examination of influence of the choice of thresholds on the conditional statistics.

Case	1	2	3	4	5	6	7
$\Gamma_{\rm th}/\langle\Gamma_{\rm C}\rangle_{\rm C}$	0.050	0.045	0.045	0.050	0.050	0.055	0.055
$C_{U\rm th}/(\langle U\rangle_{\rm C}^2/b_U)$	0.096	0.096	0.086	0.086	0.106	0.096	0.106

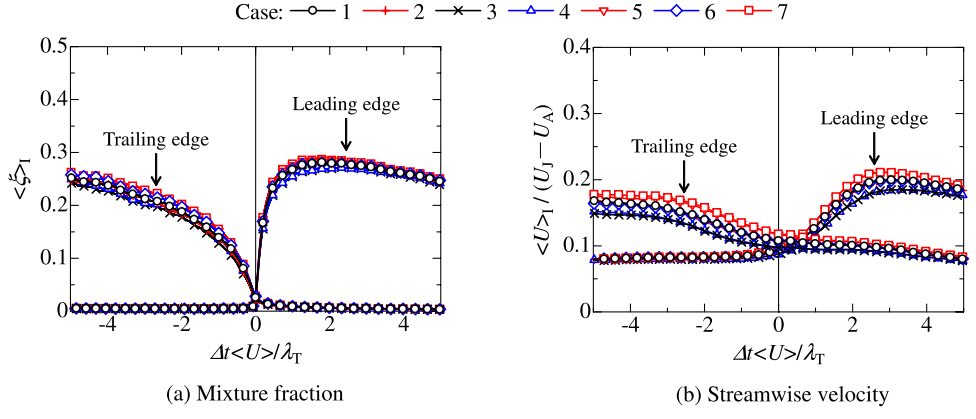

(a) Mixture fraction (b) Streamwise velocity

FIG. 13. Dependence of the conditional mean values on the choice of thresholds: (a) conditional mean concentration of nonreactive species C and (b) conditional mean streamwise velocity. The conditional statistics are calculated near the leading and trailing edges at $x/d = 20$ for the 7 choices of thresholds listed in Table I. (a) Mixture fraction. (b) Streamwise velocity.

Eqs. (2) and (4), respectively. We calculated the conditional statistics for the 7 thresholds ($\Gamma_{\rm th}, C_{U\rm th}$) listed in Table I. The thresholds for case 1 are used in this study. In the other cases, the thresholds are increased or decreased by 10% of those for case 1. Figure 13 shows the conditional average of the concentration of nonreactive species C and streamwise velocity at $x/d = 20$ calculated for various thresholds. It is found that the different thresholds do not change the overall profiles of the conditional mean values. Thus, the same conclusions can be obtained for the different thresholds listed in Table I.

[1] C. B. da Silva, J. C. R. Hunt, I. Eames, and J. Westerweel, "Interfacial layers between regions of different turbulence intensity," Annu. Rev. Fluid Mech. **46**, 567 (2014).
[2] S. Corrsin and A. L. Kistler, "Free-stream boundaries of turbulent flows," NACA Technical Report No. TN-1244, 1955.
[3] C. B. da Silva and R. R. Taveira, "The thickness of the turbulent/nonturbulent interface is equal to the radius of the large vorticity structures near the edge of the shear layer," Phys. Fluids **22**, 121702 (2010).
[4] R. R. Taveira and C. B. da Silva, "Characteristics of the viscous superlayer in shear free turbulence and in planar turbulent jets," Phys. Fluids **26**, 021702 (2014).
[5] J. Westerweel, T. Hofmann, C. Fukushima, and J. C. R. Hunt, "The turbulent/non-turbulent interface at the outer boundary of a self-similar turbulent jet," Exp. Fluids **33**, 873 (2002).
[6] J. Westerweel, C. Fukushima, J. M. Pedersen, and J. C. R. Hunt, "Mechanics of the turbulent-nonturbulent interface of a jet," Phys. Rev. Lett. **95**, 174501 (2005).
[7] J. Westerweel, C. Fukushima, J. M. Pedersen, and J. C. R. Hunt, "Momentum and scalar transport at the turbulent/non-turbulent interface of a jet," J. Fluid Mech. **631**, 199 (2009).
[8] M. Holzner, A. Liberzon, N. Nikitin, B. Lüthi, W. Kinzelbach, and A. Tsinober, "A Lagrangian investigation of the small-scale features of turbulent entrainment through particle tracking and direct numerical simulation," J. Fluid Mech. **598**, 465 (2008).
[9] M. Holzner, B. Luethi, A. Tsinober, and W. Kinzelbach, "Acceleration, pressure and related quantities in the proximity of the turbulent/non-turbulent interface," J. Fluid Mech. **639**, 153 (2009).
[10] M. Holzner and B. Lüthi, "Laminar superlayer at the turbulence boundary," Phys. Rev. Lett. **106**, 134503 (2011).
[11] C. B. da Silva and J. C. F. Pereira, "The effect of subgrid-scale models on the vortices computed from large-eddy simulations," Phys. Fluids **16**, 4506 (2004).
[12] C. B. da Silva, R. J. N. dos Reis, and J. C. F. Pereira, "The intense vorticity structures near the turbulent/non-turbulent interface in a jet," J. Fluid Mech. **685**, 165 (2011).
[13] R. R. Taveira and C. B. da Silva, "Kinetic energy budgets near the turbulent/nonturbulent interface in jets," Phys. Fluids **25**, 015114 (2013).
[14] R. R. Taveira, C. B. da Silva, and J. C. F. Pereira, "The dynamics of turbulent scalar mixing near the edge of a shear layer," J. Phys.: Conf. Ser. **318**, 052049 (2011).
[15] T. Watanabe, Y. Sakai, K. Nagata, O. Terashima, H. Suzuki, T. Hayase, and Y. Ito, "Visualization of turbulent reactive jet by using direct numerical simulation," Int. J. Model. Simul. Sci. Comput. **4**, 1341001 (2013).
[16] T. Watanabe, Y. Sakai, K. Nagata, Y. Ito, and T. Hayase, "Enstrophy and passive scalar transport near the turbulent/non-turbulent interface in a turbulent planar jet flow," Phys. Fluids **26**, 105103 (2014).
[17] T. Watanabe, Y. Sakai, K. Nagata, Y. Ito, and T. Hayase, "Vortex stretching and compression near the turbulent/nonturbulent interface in a planar jet," J. Fluid Mech. **758**, 754 (2014).
[18] T. Watanabe, Y. Sakai, K. Nagata, Y. Ito, and T. Hayase, "Wavelet analysis of coherent vorticity near the turbulent/non-turbulent interface in a turbulent planar jet," Phys. Fluids **26**, 095105 (2014).
[19] R. O. Fox, *Computational Models for Turbulent Reacting Flows* (Cambridge University Press, 2003).
[20] J. C. Hill, "Homogeneous turbulent mixing with chemical reaction," Annu. Rev. Fluid Mech. **8**, 135 (1976).
[21] R. W. Bilger, "Turbulent diffusion flames," Annu. Rev. Fluid Mech. **21**, 101 (1989).
[22] P. E. Dimotakis, "The mixing transition in turbulent flows," J. Fluid Mech. **409**, 69 (2000).
[23] T. Watanabe, Y. Sakai, K. Nagata, Y. Ito, and T. Hayase, "Reactive scalar field near the turbulent/non-turbulent interface in a planar jet with a second-order chemical reaction," Phys. Fluids **26**, 105111 (2014).
[24] S. Komori, K. Nagata, T. Kanzaki, and Y. Murakami, "Measurements of mass flux in a turbulent liquid flow with a chemical reaction," AIChE J. **39**, 1611 (1993).
[25] S. Komori, T. Kanzaki, and Y. Murakami, "Concentration correlation in a turbulent mixing layer with chemical reactions," J. Chem. Eng. Jpn. **27**, 742 (1994).
[26] A. D. Chorny and V. L. Zhdanov, "Verification of chemical reaction rate models in turbulent reacting flows at Schmidt number considerably exceeding 1," J. Eng. Phys. Thermophys. **83**, 513 (2010).
[27] V. Zhdanov and A. Chorny, "Development of macro-and micromixing in confined flows of reactive fluids," Int. J. Heat Mass Transfer **54**, 3245 (2011).
[28] A. Chorny and V. Zhdanov, "Turbulent mixing and fast chemical reaction in the confined jet flow at large Schmidt number," Chem. Eng. Sci. **68**, 541 (2012).
[29] J. Lee and R. S. Brodkey, "Turbulent motion and mixing in a pipe," AIChE J. **10**, 187 (1964).
[30] I. Nakamura, Y. Sakai, and M. Miyata, "Diffusion of matter by a non-buoyant plume in grid-generated turbulence," J. Fluid Mech. **178**, 379 (1987).
[31] T. Kubo, Y. Sakai, K. Nagata, and K. Iida, "Experimental study on the turbulent reactive plane jet in liquid," J. Fluid Sci. Technol. **4**, 368 (2009).
[32] T. Watanabe, Y. Sakai, K. Nagata, O. Terashima, and T. Kubo, "Simultaneous measurements of reactive scalar and velocity in a planar liquid jet with a second-order chemical reaction," Exp. Fluids **53**, 1369 (2012).

[33] T. Kubo, Y. Fukumura, Y. Sakai, and K. Nagata, "Study on turbulent plane jet with chemical reaction in liquid," J. Fluid Sci. Technol. **7**, 25 (2012).
[34] T. Watanabe, Y. Sakai, K. Nagata, and O. Terashima, "Joint statistics between velocity and reactive scalar in a turbulent liquid jet with a chemical reaction," Phys. Scr. **2013** (T155), 014039.
[35] T. Watanabe, Y. Sakai, K. Nagata, and O. Terashima, "Turbulent Schmidt number and eddy diffusivity change with a chemical reaction," J. Fluid Mech. **754**, 98 (2014).
[36] T. Naito, T. Watanabe, Y. Sakai, K. Nagata, O. Terashima, and Y. Ito, "Concentration measurement in a planar liquid jet with a chemical reaction by using the improved concentration measurement system based on the light absorption spectrometric method," J. Fluid Sci. Technol. **9**, JFST0041 (2014).
[37] T. Watanabe, Y. Sakai, K. Nagata, and O. Terashima, "Experimental study on the reaction rate of a second-order chemical reaction in a planar liquid jet," AIChE J. **60**, 3969 (2014).
[38] R. A. Antonia, "Conditional sampling in turbulence measurement," Annu. Rev. Fluid Mech. **13**, 131 (1981).
[39] S. B. Pope, *Turbulent Flows* (Cambridge University Press, 2000).
[40] T. B. Hedley and J. F. Keffer, "Turbulent/non-turbulent decisions in an intermittent flow," J. Fluid Mech. **64**, 625 (1974).
[41] C. B. da Silva and J. C. F. Pereira, "Invariants of the velocity-gradient, rate-of-strain, and rate-of-rotation tensors across the turbulent/nonturbulent interface in jets," Phys. Fluids **20**, 055101 (2008).
[42] M. van Reeuwijk and M. Holzner, "The turbulence boundary of a temporal jet," J. Fluid Mech. **739**, 254 (2014).
[43] M. Gampert, J. Boschung, F. Hennig, M. Gauding, and N. Peters, "The vorticity versus the scalar criterion for the detection of the turbulent/non-turbulent interface," J. Fluid Mech. **750**, 578 (2014).
[44] D. K. Bisset, J. C. R. Hunt, and M. M. Rogers, "The turbulent/non-turbulent interface bounding a far wake," J. Fluid Mech. **451**, 383 (2002).
[45] M. Gampert, V. Narayanaswamy, P. Schaefer, and N. Peters, "Conditional statistics of the turbulent/non-turbulent interface in a jet flow," J. Fluid Mech. **731**, 615 (2013).
[46] M. Gampert, K. Kleinheinz, N. Peters, and H. Pitsch, "Experimental and numerical study of the scalar turbulent/non-turbulent interface layer in a jet flow," Flow, Turbul. Combust. **92**, 429 (2014).
[47] R. K. Anand, B. J. Boersma, and A. Agrawal, "Detection of turbulent/non-turbulent interface for an axisymmetric turbulent jet: Evaluation of known criteria and proposal of a new criterion," Exp. Fluids **47**, 995 (2009).
[48] J. Philip, C. Meneveau, C. M. de Silva, and I. Marusic, "Multiscale analysis of fluxes at the turbulent/non-turbulent interface in high Reynolds number boundary layers," Phys. Fluids **26**, 015105 (2014).
[49] O. Terashima, Y. Sakai, and K. Nagata, "Simultaneous measurement of velocity and pressure in a plane jet," Exp. Fluids **53**, 1149 (2012).
[50] R. W. Bilger, L. R. Saetran, and L. V. Krishnamoorthy, "Reaction in a scalar mixing layer," J. Fluid Mech. **233**, 211 (1991).
[51] M. Wolf, M. Holzner, B. Lüthi, D. Krug, W. Kinzelbach, and A. Tsinober, "Effects of mean shear on the local turbulent entrainment process," J. Fluid Mech. **731**, 95 (2013).
[52] K. A. Buch and W. J. A. Dahm, "Experimental study of the fine-scale structure of conserved scalar mixing in turbulent shear flows. Part 1. Sc $\gg$ 1," J. Fluid Mech. **317**, 21 (1996).
[53] K. A. Buch and W. J. A. Dahm, "Experimental study of the fine-scale structure of conserved scalar mixing in turbulent shear flows. Part 2. Sc $\approx$ 1," J. Fluid Mech. **364**, 1 (1998).
[54] L. K. Su and N. T. Clemens, "Planar measurements of the full three-dimensional scalar dissipation rate in gas-phase turbulent flows," Exp. Fluids **27**, 507 (1999).
[55] L. K. Su and N. T. Clemens, "The structure of fine-scale scalar mixing in gas-phase planar turbulent jets," J. Fluid Mech. **488**, 1 (2003).
[56] J. Schumacher, K. R. Sreenivasan, and P. K. Yeung, "Very fine structures in scalar mixing," J. Fluid Mech. **531**, 113 (2005).
[57] A. Attili, J. C. Cristancho, and F. Bisetti, "Statistics of the turbulent/non-turbulent interface in a spatially developing mixing layer," J. Turbul. **15**, 555 (2014).
[58] P. S. Kothnur and N. T. Clemens, "Effects of unsteady strain rate on scalar dissipation structures in turbulent planar jets," Phys. Fluids **17**, 125104 (2005).
[59] R. W. Bilger, "Some aspects of scalar dissipation," Flow, Turbul. Combust. **72**, 93 (2004).